Hindawi Publishing Corporation
International Journal of Photoenergy
Volume 2013, Article ID 431614, 7 pages
http://dx.doi.org/10.1155/2013/431614

*Research Article*

# Surface Passivation and Antireflection Behavior of ALD $TiO_2$ on n-Type Silicon for Solar Cells

**Ing-Song Yu,[1] Yu-Wun Wang,[2] Hsyi-En Cheng,[2] Zu-Po Yang,[3] and Chun-Tin Lin[3]**

[1] *Department of Materials Science and Engineering, National Dong Hwa University, Hualien 97401, Taiwan*
[2] *Department of Electro-Optical Engineering, Southern Taiwan University of Science and Technology, Tainan 710, Taiwan*
[3] *Institute of Photonic System, National Chiao Tung University, Tainan 71150, Taiwan*

Correspondence should be addressed to Ing-Song Yu; isyu@mail.ndhu.edu.tw

Received 16 September 2013; Accepted 30 October 2013

Academic Editor: Jimmy Yu

Atomic layer deposition, a method of excellent step coverage and conformal deposition, was used to deposit $TiO_2$ thin films for the surface passivation and antireflection coating of silicon solar cells. $TiO_2$ thin films deposited at different temperatures (200°C, 300°C, 400°C, and 500°C) on FZ n-type silicon wafers are in the thickness of 66.4 nm ± 1.1 nm and in the form of self-limiting growth. For the properties of surface passivation, Si surface is effectively passivated by the 200°C deposition $TiO_2$ thin film. Its effective minority carrier lifetime, measured by the photoconductance decay method, is improved 133% at the injection level of $1 \times 10^{15}\ \mathrm{cm}^{-3}$. Depending on different deposition parameters and annealing processes, we can control the crystallinity of $TiO_2$ and find low-temperature $TiO_2$ phase (anatase) better passivation performance than the high-temperature one (rutile), which is consistent with the results of work function measured by Kelvin probe. In addition, $TiO_2$ thin films on polished Si wafer serve as good ARC layers with refractive index between 2.13 and 2.44 at 632.8 nm. Weighted average reflectance at AM1.5G reduces more than half after the deposition of $TiO_2$. Finally, surface passivation and antireflection properties of $TiO_2$ are stable after the cofire process of conventional crystalline Si solar cells.

## 1. Introduction

Most commercially available solar cells are from silicon, and p-type crystalline silicon solar cells are the mainstream now. In order to increase the efficiency of crystalline silicon solar cells, people in industry try to find the better integration processes of conventional solar cells, to improve the quality of materials, and to cost down the fabrication. Besides, new structures of silicon solar cells with higher efficiency are studied. Passivated emitter and rear, locally diffused cell (PERL), proposed by University of New South Wales, Australia, in 1994, is also one of the designs, which performs very high efficiency up to 25% [1]. In industry, the conversion efficiency of 6 inch × 6 inch p-type crystalline silicon solar cells can be over 20% using the surface passivation technology with $Al_2O_3$ thin films [2]. Unfortunately, the light induced degradation (LID) makes p-type crystalline silicon solar cells drop around 1% efficiency due to the formation of boron-oxygen clusters after light exposure [3]. Therefore, PERL with n-type silicon wafers attracts researchers' great attention recently and will dominate the crystalline Si solar cell in the near future [4, 5].

For the surface passivation and antireflection coating of p-type Si solar cells, amorphous $SiN_x$ films deposed by the technique of plasma-enhanced chemical vapor deposition (PECVD) were well developed in the early 1990s. $SiN_x$ thin films can reduce surface recombination and light reflection and additionally provide very efficient passivation for bulk defects of low cost Si materials [6, 7]. However, for the p-type diffused surface of n-type Si solar cells, $SiN_x$ dielectric coatings are not suitable for passivation, because its positive charge will decrease the properties of surface passivation. Thermal silicon oxide could be good for passivation initially, but the Si-$SiO_2$ interface on boron-diffused and undiffused surfaces degrades slowly over three months at room temperature [8, 9]. Besides, amorphous silicon (a-Si) and $Al_2O_3$ are good passivation layers but are not suitable for ARC on the front surface of solar cells. Therefore, titanium oxide ($TiO_2$) reattracts researchers' attentions, which has been used in the photovoltaic industry as an antireflection coating for many years since the 1980s due to its low growth temperature, a nontoxic and noncorrosive liquid precursor, excellent chemical resistance, an optimal reflective index, and low absorbance at wavelengths relevant to silicon solar cells. Surface passivation properties of spray pyrolysis $TiO_2$ on silicon wafer were enhanced by the formation of a $SiO_2$ layer at $TiO_2$/Si interface after being annealed at 950°C without degradation [10, 11]. Nonstoichiometric $TiO_x$ films grown by pulsed laser deposition (PLD) had some degree of passivation for nondiffused p-type Si surface through the substrate placed at the edge of plasma [12]. Recently, Thomson et al. proposed that the $TiO_2$ thin films deposited by atmospheric pressure chemical vapor deposition (APCVD) can effectively passivate n-type silicon and Boron-diffused surfaces as better as the passivation performance of $SiO_2$. These films were annealed at 300°C in $N_2$ ambient and light soaked by halogen lamp to create negative charges for better surface passivation [8].

Many technologies can be employed to grow $TiO_2$ thin films, such as PECVD, APCVD, PLD, spray pyrolysis, reactive sputtering, and sol-gel [13]. In this paper, we grew $TiO_2$ thin films on Si wafers by atomic layer deposition (ALD) which performs excellent uniformity, accurate thickness control, and almost 100% step coverage on substrate surface [14]. Some characterization of $TiO_2$ thin films by ALD will be shown. An investigation of the surface passivation and antireflection coating on silicon relative to the growth temperatures of ALD will be discussed. The degradation and influence of cofire process for the metallization of Si solar cells will also be studied. This work is essential for the applications of ALD $TiO_2$ thin films in n-type crystalline silicon solar cells.

## 2. Experiment

In the experiment, we used n-type double-polished FZ silicon wafers with resistivity 1000 Ω-cm, thickness 500 $\mu$m, and orientation (100). Before the deposition of $TiO_2$, the cleanness of Si wafers was conducted by acetone to remove the organics and 5% hydrofluoric acid to remove the native oxide. Then, wafer was rinsed in deionized water and dried with $N_2$ gas. Right after the cleaning, Si substrate was placed in the reaction chamber of our ALD system which is shown in Figure 1. Until the base pressure of chamber reached $2 \times 10^{-2}$ torr, we set the deposition temperature as 200°C, 300°C, 400°C, and 500°C, respectively. For the deposition process of $TiO_2$ thin films, we employed $TiCl_4$ and $H_2O$ as reactants and Ar (99.999%) as purging gas. The injection volume of $TiCl_4$ and $H_2O$ was 0.10 cc and 0.06 cc, respectively, for each step according to the ideal gas law. One cycle of a monolayer deposition included eight steps ($TiCl_4$ reactant, pump-down, Ar purge, pump-down, $H_2O$ reactant, pump-down, Ar purge, and pump-down), and it took eight seconds. After 1000-cycle deposition and cool-down to room temperature of the chamber, n-type FZ Si wafer with double-side $TiO_2$ coating was done for further analysis [15]. First, the characterization of $TiO_2$ films was made by scanning electron microscopy (SEM) and X-ray diffraction (XRD). Second, the study of surface passivation for ALD $TiO_2$ on n-type FZ silicon wafers was carried out by Sinton's quasi-steady-state photoconductance (QSSPC) method and Kelvin probe for work function measurement [16, 17]. Finally, optical properties of $TiO_2$ thin films were decided by the spectroscopic ellipsometry measurement and reflection spectroscopy in the wavelength range of 300 nm–1200 nm.

Table 1: Estimation of grain size of $TiO_2$ thin films by SEM and XRD.

| | ALD 200°C | ALD 300°C | ALD 400°C | ALD 500°C |
|---|---|---|---|---|
| Grain size from SEM (nm) | 110 | 70 | 45 | 70 |
| Grain size from XRD (nm) | 39 | 31 | 22 | 25 |

## 3. Results and Discussions

*3.1. The Characterization of ALD $TiO_2$ Thin Films.* The surface morphology and cross-section of our $TiO_2$ thin films were observed by a JSM-6700F SEM with accelerating voltage 10 kV. In Figure 2, SEM images of $TiO_2$ thin films deposited at different temperatures show that these films are polycrystalline and have grain sizes in the range of 45 nm and 110 nm. Cross-section SEM images, in the inset of Figure 3, were used to decide the thickness of $TiO_2$ thin films. The thickness of $TiO_2$ thin films is 66.4 nm ± 1.1 nm for all growth temperatures shown in Figure 3. Here, we can find that the growth rate is independent of the substrate's temperature, which indicates that the reaction is self-limited by the saturated surface adsorption of reactants. The adsorption thickness, 0.066 nm, is almost the same for each cycle of ALD process. Our ALD system demonstrates very large growth windows for the $TiO_2$ thin films deposited on Si wafers.

The crystallinity of ALD $TiO_2$ thin films at different temperatures was studied by Bruker X-ray diffractometry. In Figure 4, XRD patterns demonstrate that $TiO_2$ thin films deposited at low temperatures are primarily with anatase phase. As the deposition temperature increased up to 500°C, rutile phase began to be obtained in $TiO_2$ thin films. When the $TiO_2$ films are annealed with the parameter of 900°C, 60 seconds, and $O_2$ ambient, rutile phase dominated in the films. Rapid thermal annealing (RTA) induces phase transformation of $TiO_2$ films from low-temperature anatase phase to high-temperature rutile phase. The higher RTA temperature is, the more rutile phase we observe. From this work, we can control the phase of $TiO_2$ thin films for the following studies of surface passivation and antireflection coating on n-type Si.

In addition, grain size of ALD $TiO_2$ can be estimated by SEM images and Scherrer equation of XRD, which is summarized in Table 1. We get smaller grain size by XRD than the one by SEM, but their trends are the same at different deposition temperatures. For $TiO_2$ films only with anatase phase (at deposition temperatures 200°C, 300°C, and 400°C), the lower deposition temperature we set, the larger grain size we observe. According to the growth mechanism of $TiO_2$ thin films, higher-temperature deposition results in significant

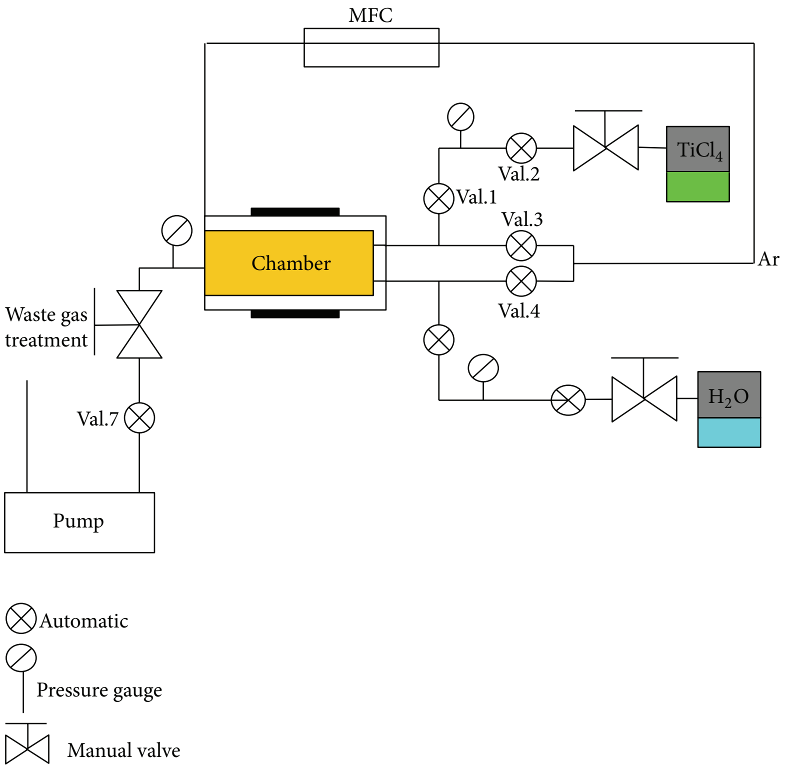

Figure 1: Schematic of the ALD system.

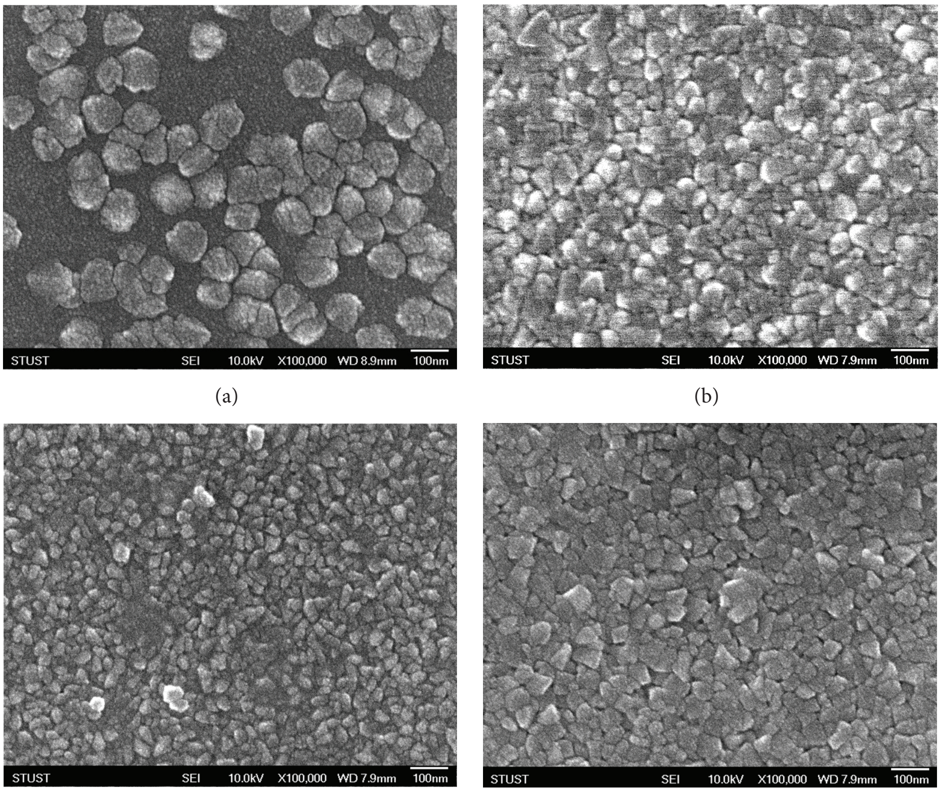

(a) (b) (c) (d)

Figure 2: SEM images of $TiO_2$ thin films at different growth temperatures: (a) 200°C, (b) 300°C, (c) 400°C, and (d) 500°C.

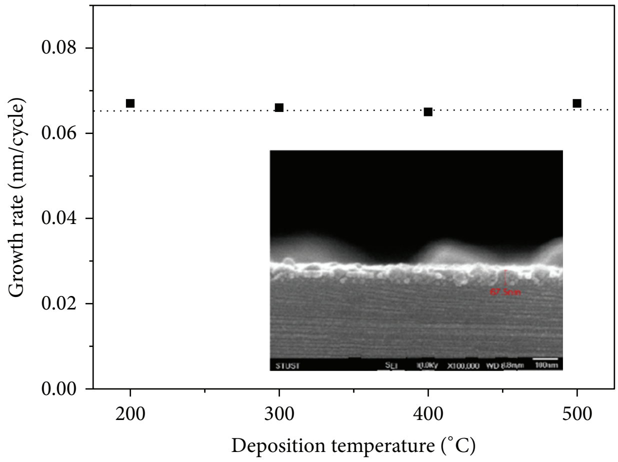

Figure 3: ALD $TiO_2$ growth rate at temperature 200°C, 300°C, 400°C, and 500°C is 0.066 nm per cycle due to self-limiting growth. Inset is the cross-section SEM image.

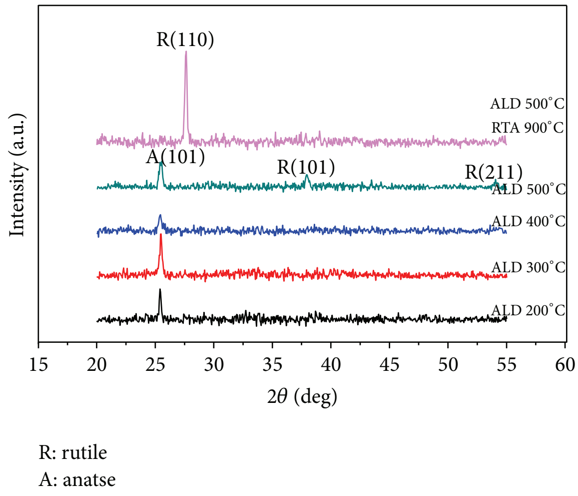

Figure 4: XRD patterns of $TiO_2$ thin films deposited at 200°C, 300°C, 400°C, 500°C, and RTA 900°C.

grain refinement, due to an increased density of sites for nucleation of crystallization [18]. As the deposition temperature increases up to 500°C, we find the phase transformation to rutile and the effect of grain growth, which could influence the surface passivation of $TiO_2$ thin film on n-type Si.

*3.2. Surface Passivation Properties of ALD $TiO_2$.* Sinton's WCT-120, a photoconductance decay method, was employed to measure the effective minority carrier lifetime of samples. The effective lifetime ($\tau_{\text{eff}}$) is a combination of bulk lifetime ($\tau_{\text{bulk}}$) and surface lifetime ($\tau_{\text{sur}}$) as follows:

$$\frac{1}{\tau_{\text{eff}}} = \frac{1}{\tau_{\text{bulk}}} + \frac{1}{\tau_{\text{sur}}}, \qquad \frac{1}{\tau_{\text{sur}}} = \frac{2S}{W}, \tag{1}$$

where $W$ is the sample thickness and $S$ is surface recombination velocity. In order to study the surface passivation of ALD $TiO_2$ thin films, we used FZ n-type Si substrate which has very large bulk lifetime. Therefore, the effective lifetime measured is close to surface lifetime to calculate the surface recombination velocity. Figure 5 shows the effective lifetime as function of minority carrier density by WCT-120. The effective lifetime without ALD $TiO_2$ passivation is 9.2 $\mu$s at the injection level of $1 \times 10^{15}$ $cm^{-3}$ ($S = 2717$ cm/s). After the deposition of $TiO_2$ at 200°C, the effective lifetime is 21.5 $\mu$s at the injection level of $1 \times 10^{15}$ $cm^{-3}$ ($S = 1163$ cm/s). Si surface is effectively passivated by the ALD $TiO_2$ thin films, especially for the one deposited at the low temperature. At the deposition temperature 500°C, when rutile phase can be observed, the degree of surface passivation does not exist anymore. For the samples with RTA 900°C, their effective lifetimes are very low (not shown). From the results of the effective lifetime measurement, we can find that $TiO_2$ thin film deposited at 200°C has the best performance for surface passivation on n-type Si.

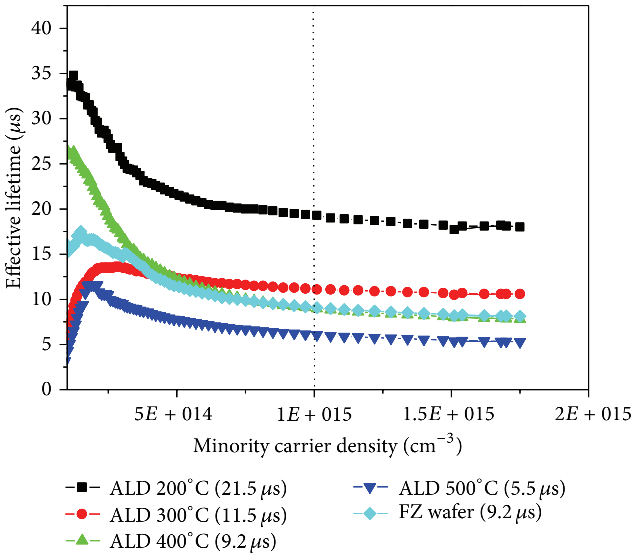

Figure 5: Effective minority carrier lifetime as function of carrier density at different deposition temperatures and their lifetime values at injection level $1 \times 10^{15}$ $cm^{-3}$.

Moreover, we study the degradation and influence of metallization process in crystalline solar cells. In Figure 6, the effective lifetime of 30 nm $TiO_2$ thin film grown at temperature 200°C slightly increased after five months of deposition. After cofire process of belt-type furnace at peak temperature 800°C, the effective lifetime decreased a little but is still good enough for surface passivation. We can summarize that ALD $TiO_2$ thin films have high stability for the applications in crystalline silicon solar cells.

In the study of solar cells, work function is sensitive to the voltage across the barrier of p-n junction and the surface traps in the passivation emitter interface. In this work, nonscanning ambient Kelvin probe, KP 020, was used to measure the work function of $TiO_2$ thin films at different deposition temperatures. In Figure 7, the higher deposition temperature we use, the larger work function of $TiO_2$ we measure, which is consistent with the result of effective

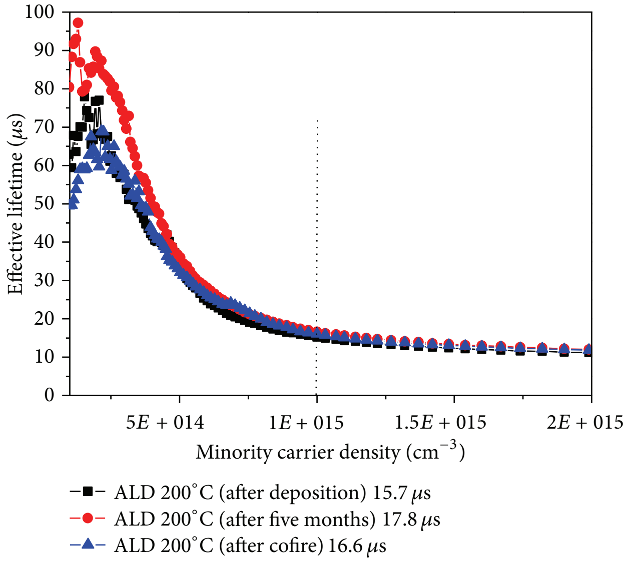

FIGURE 6: Effective minority carrier lifetime of 30 nm $TiO_2$ thin films deposited at 200°C in three cases: after deposition, five months, and cofire.

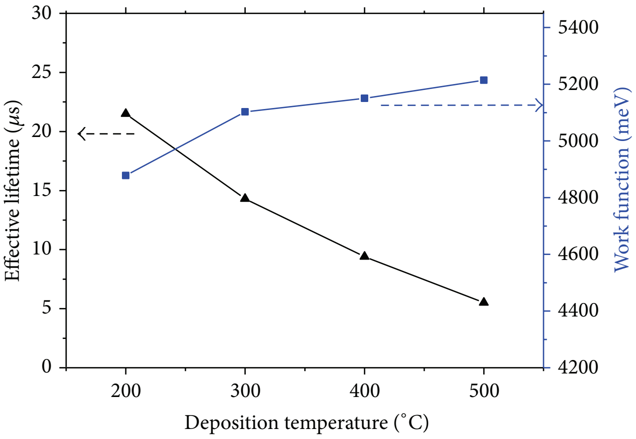

FIGURE 7: Work function (■) and effective lifetime (▲) of $TiO_2$ thin films at different deposition temperatures.

lifetimes at different deposition temperatures. To explain this, we can see the energy band diagram of $TiO_2$ and Si in Figure 8. $TiO_2$/Si heterojunction makes energy band bending at the interface of $TiO_2$ and n-type Si [19]. According to the work function of $TiO_2$ thin films we measured, more band bending occurred in the case of $TiO_2$ film deposited at 500°C, which induce more recombination at the interface and lower effective lifetime of samples.

*3.3. Optical Properties of ALD $TiO_2$.* Now we will demonstrate that our ALD $TiO_2$ thin films are an excellent antireflection coating layer for crystalline silicon solar cells. For the conventional quarter-wavelength antireflection coating (ARC), the refractive index of coating layer has to be chosen as $\sqrt{n_s}$, where $n_s$ is the refractive index of substrate, that is, Si in this case. For example, considering the refractive index of Si in the spectral ranges of 400 nm–800 nm [20], the refractive index of quarter-wavelength ARC thin films should be in the range of ~2.36–1.92. To verify this, we performed the spectroscopic ellipsometry measurements and extracted the refractive index of our ALD $TiO_2$ thin films. Figure 9 shows the refractive index as function of wavelength for our $TiO_2$ thin film deposited at temperature 200°C. Its refractive index decreases monotonically from 2.65 to 2.25 as wavelength decreases from 375 nm to 900 nm, showing a similar trend as anatase-phase bulk $TiO_2$ [21] but having a little lower value of index, which probably is because of polycrystal structure in our films (see SEM images in Figure 2). Most importantly, the results show that our ALD $TiO_2$ thin films are an excellent choice of quarter-wavelength ARC layer for Si solar cells.

To further prove this, we used Hitachi U-4100 to measure the reflectance spectra of our ALD $TiO_2$ thin films and a Si wafer as a reference, shown in Figure 10. Firstly, all of $TiO_2$ deposited Si wafers show a much lower reflectance than those of a bare Si wafer over the measured spectral range. Secondly, a minimum reflectance of $TiO_2$ deposed Si wafers is observed at ~550 nm, which is consistent with the requirement of film thickness for quarter-wavelength ARC; that is, $d = \lambda/4n_{\mathrm{TiO_2}}$. Taking $\lambda = 550$ nm and $n_{\mathrm{TiO_2}} \approx 2.15$, we have $d = 64$ nm, which agrees with our SEM results. Again, this indicates that our $TiO_2$ thin films serve as an ARC layer. Thirdly, the reflectance of all $TiO_2$ deposited Si increases monotonically from ~550 nm to ~1000 nm. This is because the thickness (66.4 nm) of our $TiO_2$ film deviates the $d = \lambda/4n_{\mathrm{TiO_2}}$ further and further as wavelength increases. Fourthly, a bump rising at around 1000 nm is observed for all samples. This is because the reflectance from Si backside surface starts to contribute the measured reflectance as wavelength approaching the band gap wavelength of Si.

To overall justify the ARC performance of our $TiO_2$ thin films for solar cells, we calculate the weight average reflectance (WAR) at AM1.5G in the range of 300 nm to 1200 nm. The results show that all of our ALD $TiO_2$ thin films have WAR (16.68%–18.92%) less than the half of WAR (38.36%) of bare Si. The $TiO_2$ thin film grown at 200°C shows the lowest value of WAR because it has the lowest refractive index deduced from ellipsometry. A lower WAR value can be achieved with optimized growth conditions and film thickness. Moreover, the reflectance spectra as well as the WAR are almost the same after cofire process by belt-type furnace at peak temperature 800°C (not shown), which indicates that our ALD $TiO_2$ thin films are suitable for the fabrication processes of crystalline silicon solar cells.

## 4. Conclusion

Growth window of self-limiting can be from 200°C to 500°C in our $TiO_2$ ALD system with the growth rate 0.066 nm per cycle. All these films are excellent antireflection coating layers for Si. For lower deposition temperature of $TiO_2$ thin films, we find smaller energy band bending in the interface of $TiO_2$/Si and better surface passivation performance. The best surface passivation and antireflection coating on Si wafers are carried out at the deposition temperature 200°C, mainly

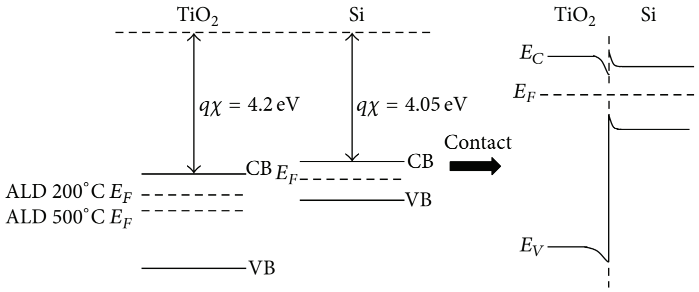

FIGURE 8: The left hand side is energy band diagrams of TiO$_2$ and Si before contact. After contact, band bending occurs at the interface of TiO$_2$ and Si.

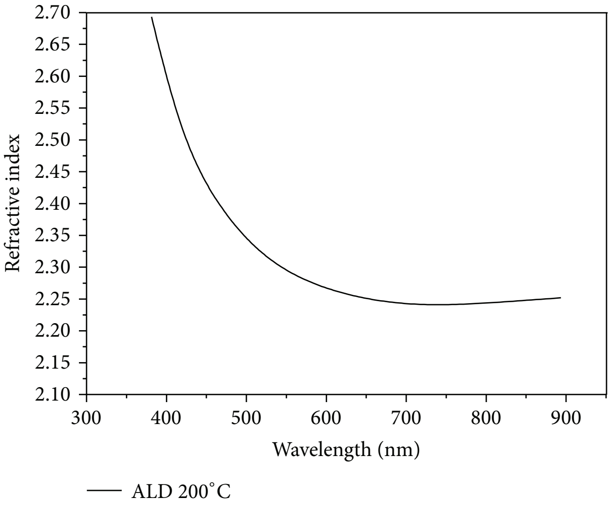

FIGURE 9: Refractive index as function of wavelength for TiO$_2$ thin film grown at 200°C.

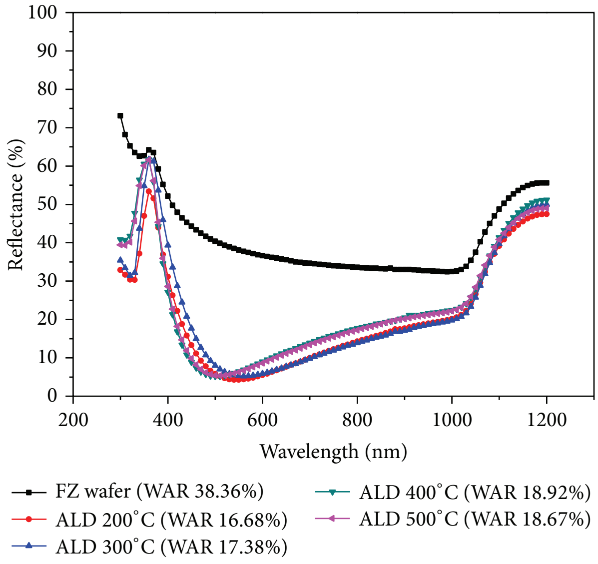

FIGURE 10: Reflectance of bare Si wafer and Si with TiO$_2$ thin films grown at different temperatures as function of wavelength from 300 nm to 1200 nm.

anatase phase in TiO$_2$ film. Once the rutile appears via high-temperature depositions or annealing processes, the degree of surface passivation will not exist. After the cofire process of conventional crystalline Si solar cells, we prove that their surface passivation and antireflection properties are very stable, which can be applied for n-type crystalline silicon solar cells.

## Conflict of Interests

The authors declare that there is no conflict of interests regarding the publication of this paper.

## Acknowledgments

The authors acknowledge National Science Council of Taiwan (NSC 101-2218-E-259-001) for financially supporting this study and E-Ton Solar Tech. Co., Ltd., for the measurement of Sinton WCT-120 and Hitachi U-4100.

## References

[1] M. A. Green, J. Zhao, and A. Wang, "23% module and other silicon solar cell advances," in *Proceedings of 2nd World Conference on Photovoltaic Energy Conversion*, vol. 1187, 1998.

[2] F. Werner, B. Veith, V. Tiba et al., "Very low surface recombination velocities on p—and n-type c-Si by ultrafast spatial atomic layer deposition of aluminum oxide," *Applied Physics Letters*, vol. 97, no. 16, Article ID 162103, 2010.

[3] K. Bothe, R. Sinton, and J. Schmidt, "Fundamental boron-oxygen-related carrier lifetime limit in mono- and multicrystalline silicon," *Progress in Photovoltaics*, vol. 13, no. 4, pp. 287–296, 2005.

[4] J. Zhao and A. Wang, "Rear emitter n-type passivated emitter, rear totally diffused silicon solar cell Structure," *Applied Physics Letters*, vol. 88, no. 24, Article ID 242102, 2006.

[5] B. G. Lee, J. Skarp, V. Malinen, S. Li, S. Choi, and H. M. Branz, "Excellent passivation and low reflectivity Al$_2$O$_3$/TiO$_2$ bilayer coating for n-wafer silicon solar cells," in *Proceedings of 38th IEEE Photovoltaic Specialists Conference (PVSC '12)*, 2012.

[6] A. G. Aberle, "Surface passivation of crystalline silicon solar cells: a review," *Progress in Photovoltaics*, vol. 8, pp. 473–487, 2000.

[7] E. Fourmond, G. Dennler, R. Monna, M. Lemiti, A. Fave, and A. Laugier, "UVCVD silicon nitride passivation and ARC layers

for multicrystalline solar cells," *Solar Energy Materials and Solar Cells*, vol. 65, no. 1, pp. 297–301, 2001.

[8] A. F. Thomson, S. Z. Lynn, and K. R. McIntosh, "Passivation of silicon by negatively charged $TiO_2$," in *Proceedings of 25th European Photovoltaic Solar Energy Conference and Exhibition (EUPVSEC '05)*, vol. 1146, 2010.

[9] A. F. Thomson and K. R. Mclntosh, "Degradation of oxide-passivated boron-diffused silicon," *Applied Physics Letters*, vol. 95, Article ID 052101, 2009.

[10] B. S. Richards, J. E. Cotter, and C. B. Honsberg, "Enhancing the surface passivation of $TiO_2$ coated silicon wafers," *Applied Physics Letters*, vol. 80, no. 7, pp. 1123–1125, 2002.

[11] B. S. Richards, "Single-material $TiO_2$ double-layer antireflection coatings," *Solar Energy Materials and Solar Cells*, vol. 79, no. 3, pp. 369–390, 2003.

[12] L. M. Doeswijk, H. H. C. De Moor, D. H. A. Blank, and H. Rogalla, "Passivating $TiO_2$ coatings for silicon solar cells by pulsed laser deposition," *Applied Physics A*, vol. 69, no. 7, pp. S409–S411, 1999.

[13] P. Vitanov, G. Agostinelli, A. Harizanova et al., "Low cost surface passivation for p-type mc-Si based on pseudobinary alloys $(Al_2O_3)_x(TiO_2)_{1-x}$," *Solar Energy Materials and Solar Cells*, vol. 90, no. 15, pp. 2489–2495, 2006.

[14] S. M. George, "Atomic layer deposition: an overview," *Chemical Reviews*, vol. 110, no. 1, pp. 111–131, 2010.

[15] H.-E. Cheng, C.-M. Hsu, and Y.-C. Chen, "Substrate materials and deposition temperature dependent growth characteristics and photocatalytic properties of ALD $TiO_2$ films," *Journal of the Electrochemical Society*, vol. 156, no. 8, pp. D275–D278, 2009.

[16] A. Cuevas and D. Macdonald, "Measuring and interpreting the lifetime of silicon wafers," *Solar Energy*, vol. 76, no. 1–3, pp. 255–262, 2004.

[17] K. Dirscherl, I. Baikie, G. Forsyth, and A. Van der Heide, "Utilisation of a micro-tip scanning Kelvin probe for non-invasive surface potential mapping of mc-Si solar cells," *Solar Energy Materials and Solar Cells*, vol. 79, no. 4, pp. 485–494, 2003.

[18] D. R. G. Mitchell, D. J. Attard, and G. Triani, "Transmission electron microscopy studies of atomic layer deposition $TiO_2$ films grown on silicon," *Thin Solid Films*, vol. 441, no. 1-2, pp. 85–95, 2003.

[19] S. M. Sze and K. K. Ng, *Physics of Semiconductor Devices*, 2nd edition, 1981.

[20] E. D. Palik, *Handbook of Optical Constants of Solids*, vol. 1, 1991.

[21] G. E. Jellison Jr., L. A. Boatner, J. D. Budai, B.-S. Jeong, and D. P. Norton, "Spectroscopic ellipsometry of thin film and bulk anatase $(TiO_2)$," *Journal of Applied Physics*, vol. 93, no. 12, pp. 9537–9541, 2003.